

1 **Title:** Hypertriglyceridemia as a Key Contributor to Abdominal Aortic Aneurysm  
2 Development and Rupture: Insights from Genetic and Experimental Models

3  
4 **Author:** Yaozhong Liu<sup>1</sup>, Huilun Wang<sup>1,2</sup>, Minzhi Yu<sup>3</sup>, Lei Cai<sup>4</sup>, Ying Zhao<sup>1</sup>, Yalun  
5 Cheng<sup>1</sup>, Yongjie Deng<sup>1</sup>, Yang Zhao<sup>1</sup>, Haocheng Lu<sup>5</sup>, Xiaokang Wu<sup>1</sup>, Guizhen Zhao<sup>1,6</sup>,  
6 Chao Xue<sup>1,7</sup>, Hongyu Liu<sup>1</sup>, Ida Surakka<sup>1</sup>, Anna Schwendeman<sup>3</sup>, Hong S. Lu<sup>4</sup>, Alan  
7 Daugherty<sup>4</sup>, Lin Chang<sup>1</sup>, Jifeng Zhang<sup>1</sup>, Ryan E. Temel<sup>4,\*</sup>, Y. Eugene Chen<sup>1,8,\*</sup>, Yanhong  
8 Guo<sup>1,\*</sup>

9  
10 <sup>1</sup>Department of Internal Medicine, Frankel Cardiovascular Center, University of Michigan  
11 Medical Center, Ann Arbor, Michigan, USA.

12 <sup>2</sup>Department of Molecular Physiology and Biological Physics, University of Virginia  
13 School of Medicine, Charlottesville, Virginia, USA.

14 <sup>3</sup>Department of Pharmacology, University of Michigan, Ann Arbor, Michigan, USA.

15 <sup>4</sup>Saha Cardiovascular Research Center and Department of Physiology, College of  
16 Medicine, University of Kentucky, Lexington, Kentucky 40536.

17 <sup>5</sup>Department of Pharmacology, Southern University of Science and Technology,  
18 Guangdong, China.

19 <sup>6</sup>College of Pharmacy Health, University of Houston, Houston, Texas, USA.

20 <sup>7</sup>Department of Internal Medicine, Rochester General Hospital, Rochester, New York,  
21 USA.

22 <sup>8</sup>Center for Advanced Models for Translational Sciences and Therapeutics, University of  
23 Michigan Medical Center, Ann Arbor, Michigan, USA.

24  
25 Total word count: 8255

26  
27 **\* To whom correspondence should be addressed:**

28 Yanhong Guo, M.D., Ph.D., Department of Internal Medicine, University of Michigan  
29 Medical Center, Ann Arbor, MI 48109, Phone: 734-764-1405, Email:  
30 [yanhongg@umich.edu](mailto:yanhongg@umich.edu)

31 Or

32 Y. Eugene Chen, M.D., Ph.D., Department of Internal Medicine, University of Michigan  
33 Medical Center, Ann Arbor, MI 48109, USA. Phone: 734-936-9548, Email:  
34 [echenum@umich.edu](mailto:echenum@umich.edu)

35 Or

36 Ryan E. Temel, Ph.D., Saha Cardiovascular Research Center and Department of  
37 Physiology, College of Medicine, University of Kentucky, Lexington, KY 40536, USA.  
38 Phone: 859-218-1706, Email: [ryan.temel@uky.edu](mailto:ryan.temel@uky.edu)

39

40 **Abstract:**

41 Abdominal aortic aneurysm (AAA) is a life-threatening vascular disease without effective  
42 medications. This study integrated genetic, proteomic, and metabolomic data to identify  
43 causation between increased triglyceride (TG)-rich lipoproteins and AAA risk. Three  
44 hypertriglyceridemia mouse models were employed to test the hypothesis that  
45 increased plasma TG concentrations accelerate AAA development and rupture. In the  
46 angiotensin II-infusion AAA model, most *Lpl*-deficient mice with severely high plasma  
47 TG concentrations died of aortic rupture. Consistently, *Apoa5*-deficient mice with  
48 moderately increased TG concentrations had accelerated AAA development, while  
49 human *APOC3* transgenic mice with dramatically increased TG concentrations exhibited  
50 aortic dissection and rupture. Increased TG concentrations and palmitate inhibited lysyl  
51 oxidase maturation. Administration of antisense oligonucleotide targeting *Angptl3*  
52 profoundly inhibited AAA progression in human *APOC3* transgenic mice and *ApoE*-  
53 deficient mice. These results indicate that hypertriglyceridemia is a key contributor to  
54 AAA pathogenesis, highlighting the importance of triglyceride-rich lipoprotein  
55 management in treating AAA.

56

57

## 58 Introduction

59 Abdominal aortic aneurysm (AAA) is a progressive vascular disease characterized by  
60 the localized enlargement of the abdominal aorta. The prevalence of AAA is estimated  
61 to be as high as 8% in men and 2% in women over 65 years of age.<sup>1</sup> Most AAAs are  
62 asymptomatic, but the mortality rate is up to 80% if rupture occurs.<sup>2</sup> As maximum aortic  
63 diameter is the most established predictor of aneurysm rupture, current guidelines  
64 recommend considering surgical repair for asymptomatic AAA patients when maximal  
65 aortic diameter is  $\geq 50$  mm in women and  $\geq 55$  mm in men. Open surgical or  
66 percutaneous endovascular aneurysm repair is still the only therapeutic option.<sup>3</sup>  
67 Patients with AAA smaller than these thresholds are typically monitored through imaging  
68 surveillance. AAA-relevant risk factors, including smoking, male sex, aging,  
69 hypertension, and hyperlipidemia, are associated with enhanced aneurysm formation  
70 and growth. Currently, medications to reduce AAA risk factors, such as angiotensin II  
71 (AngII) receptor antagonists, beta-adrenoceptor blockers, statins, and anticoagulants,  
72 have not been proven effective in halting the growth of an aneurysm or preventing the  
73 rupture of asymptomatic AAA based on the findings from randomized controlled trials.<sup>4,5</sup>

74  
75 Our recent comprehensive genome-wide association studies (GWAS) meta-analysis,  
76 which included approximately 40,000 individuals with AAAs and over 1 million  
77 individuals without AAAs, has demonstrated that one-third of the lead variants at the  
78 121 genome-wide significant AAA risk loci are associated with major lipid fractions, such  
79 as total cholesterol (TC), triglycerides (TG), low-density lipoprotein cholesterol (LDL-C),  
80 or high-density lipoprotein cholesterol (HDL-C).<sup>6</sup> Other genetic association studies have  
81 identified that a 1-standard deviation increase in TG concentrations is associated with a  
82 69% higher risk of AAA.<sup>7,8</sup> Population-based studies have reported that individuals with  
83 increased serum very low-density lipoprotein-cholesterol (VLDL-C) and TG  
84 concentrations are more likely to develop larger AAA sizes and have a higher risk of  
85 rupture.<sup>9,10</sup> These epidemiologic and genetic findings suggest that increased TG-rich  
86 lipoproteins (TRL) may accelerate AAA development and rupture, and modulating TG  
87 concentrations or metabolites may become new therapeutic strategies for AAA.

88  
89 TG, also known as triacylglycerols (TAG), are composed of glycerol and fatty acids and  
90 are the most abundant lipids in the body. Chylomicrons transport dietary triglycerides  
91 from the small intestines, and VLDLs transport endogenously synthesized triglycerides  
92 from the liver to peripheral tissues, such as the heart, skeletal muscle, and adipose  
93 tissues. Triglyceride metabolism is a complex process involving the breakdown and  
94 utilization of this lipid. Several proteins and enzymes play critical roles in regulating  
95 triglyceride metabolism.<sup>11</sup> Among these, lipoprotein lipase (LPL), ApoC-III

96 (apolipoprotein C-III, APOC3), ApoC-II, ApoA-V (apolipoprotein A5, APOA5), and  
97 angiopoietin-like proteins (ANGPTL3, ANGPTL4, and ANGPTL8) are key players. LPL is  
98 a critical enzyme that facilitates the hydrolysis of triglycerides carried by chylomicrons  
99 and VLDL into free fatty acids (FFA) and glycerol, allowing them to be utilized by various  
100 cells for energy or storage. Our previous study found that an intronic LPL variant,  
101 associated with increased LPL expression, was strongly related to reduced plasma TG  
102 concentrations and AAA risk.<sup>6</sup> APOA5 is almost exclusively expressed in the liver and  
103 secreted in conjunction with VLDL particles. ApoC-III is a constituent of chylomicrons  
104 and VLDL particles and inhibits LPL activity, while ApoA-V and ApoC-II enhance LPL  
105 activity and promote the clearance of TG-rich lipoproteins. ANGPTL3 and ANGPTL8 are  
106 secreted proteins and inhibitors of LPL-mediated plasma TG clearance. In numerous  
107 studies involving humans and animals, loss-of-function of APOC2 or APOA5 is  
108 associated with increased plasma concentrations of TG and chylomicronemia.<sup>12,13</sup>  
109 Among the putatively causal circulating proteins associated with AAA, we observed that  
110 higher APOA5 expression is associated with decreased AAA risk.<sup>6</sup> Conversely, gene  
111 silencing of APOC3 or ANGPTL3 significantly reduced TG and TC concentrations,  
112 making this method an effective strategy for lowering plasma lipids and preventing  
113 cardiovascular diseases.<sup>14-17</sup> In the present study, we demonstrated that increased TG-  
114 rich lipoproteins accelerate AAA formation and rupture, and we provide evidence that  
115 effective management of plasma TG concentrations can alleviate AAA progression.

116

## 117 **Methods**

118 A detailed description of the methods is available in the Supplemental Materials. All  
119 animal procedures followed the protocols approved by the Institutional Animal Care &  
120 Use Committee (IACUC) at the University of Michigan and University of Kentucky.

121

## 122 **Statistic analysis**

123 Analyses of RNA sequencing and genetic data were performed using R language  
124 (v4.3.0). Statistical analyses of other data were conducted using GraphPad Prism 10.  
125 Most of the data are presented as mean  $\pm$  standard error of the mean (SEM). The  
126 distribution of data was assessed using the Kolmogorov-Smirnov test (for  $n > 4$ ) or the  
127 Shapiro-Wilk test (for  $n \leq 4$ ). For normally distributed data, Student's t-tests were used  
128 to compare two groups, one-way analysis of variance (ANOVA) was used to compare  
129 multiple groups, and the Sidak method was applied for multiple comparison correction.  
130 For non-normally distributed data, Mann-Whitney U tests were used to compare two  
131 groups, Kruskal-Wallis tests were employed to compare multiple groups, and the Dunn  
132 method was used for multiple comparisons correction. A P-value less than 0.05 was  
133 considered statistically significant.

## 134 Results

### 135 Genetic, proteomic, and metabolic studies underscore high triglyceride-rich 136 lipoproteins as a causal risk factor for AAA.

137 Genetic variants that modulate the expression of genes encoding the candidate proteins  
138 or the abundances of metabolites represent valuable tools for guiding therapeutic  
139 strategies. Recent studies have identified cis-acting protein quantitative trait loci (cis-  
140 pQTL) that can be used as instrumental variables (IVs) for inferring causality.<sup>18,19</sup>  
141 Combining cis-pQTL and GWAS findings, we performed Mendelian randomization (MR)  
142 analyses to assess the causal effects of circulating proteins on AAA risk and identified  
143 that 41 out of 2,698 circulating proteins were significantly associated with AAA after  
144 adjusting for multiple tests (Fig 1, full MR results in Supplementary Table 1). Among  
145 them, genetically determined circulating APOC3 (OR=1.84) and APOA5 (OR=0.61) had  
146 the most significant effects on AAA risk. Seven of the 41 circulating proteins, including  
147 APOC3, APOA5, LPL, APOE, PLTP (phospholipid transfer protein), PCSK9 (proprotein  
148 convertase subtilisin/kexin type 9), and LPA (lipoprotein(A)), play an important role in  
149 lipid metabolism, especially in VLDL and chylomicron metabolism (Fig 1B). Our previous  
150 GWAS findings demonstrated that 42 lead variants at the AAA risk loci are associated  
151 with major lipid fractions.<sup>6</sup> After prioritizing the role of five major lipoprotein components  
152 (HDL-C, LDL-C, TG, APOA1, and APOB) as risk factors for AAA, TG was the top-ranked  
153 risk factor for AAA with a marginal inclusion probability of 0.81 (P=0.007; Supplementary  
154 Table 2). Consistent with previous studies,<sup>6-8</sup> LDL-C, HDL-C, and APOA1 were  
155 significant factors (Supplementary Table 2). These genetic and proteomic findings  
156 indicate that TG-related metabolism may play a substantial role in AAA pathogenesis.

157  
158 To further identify genetic associations between AAA risk loci and circulating metabolic  
159 traits, we utilized the data from a recently published GWAS study of 233 circulating  
160 metabolites to perform a two-sample MR analysis.<sup>20</sup> The NMR-measured metabolites  
161 included 213 lipid traits (lipids, lipoproteins, and fatty acids) and 20 non-lipid traits  
162 (amino acids, ketone bodies, and glucose/glycolysis-related metabolites).<sup>20</sup> Lipoproteins  
163 are classified by particle sizes (XXL, XL, L, M, S, and XS) and then subgrouped by the  
164 components (particle number, phospholipids, cholesterol, cholesterol ester, free  
165 cholesterol, and TG). For each metabolite, we used the inverse variance-weighted  
166 (IVW) method as the primary MR approach and MR-Egger analysis and weighted  
167 median-based regression methods as sensitivity analyses. We demonstrated that TG-  
168 rich lipoproteins, including VLDL, IDL (intermediate density lipoprotein), and LDL, and all  
169 the components in TRL particles, were positively associated with AAA risk, while HDL  
170 and glucose were negatively associated with AAA risk, consistent with population  
171 findings (Fig 1C, full MR results in Supplementary Table 3).<sup>9,10,21,22</sup> Interestingly, we

172 noticed that TG component of HDL was positively associated with AAA risk compared to  
173 other components in HDL particles, such as cholesterol and phospholipids (Fig 1C).  
174 Concomitantly, we observed that total fatty acid and saturated fatty acid, the metabolites  
175 of triglycerides, were also positively associated with AAA risk. These findings raise the  
176 possibility that lowering triglycerides and related metabolites could provide a therapeutic  
177 pathway for reducing the risk of AAA.

178

### 179 **Impaired LPL activity accelerates AAA development and rupture.**

180 Chronic subcutaneous infusion of AngII serves as a well-established AAA model in mice  
181 under hypercholesterolemic conditions, which includes using mice with deficiencies in  
182 apolipoprotein E (*ApoE*) or LDL receptor (*Ldlr*) or manipulating by adeno-associated  
183 virus-mediated overexpression of *Pcsk9* to induce hyperlipidemia.<sup>23-25</sup> Our previous  
184 GWAS demonstrated that LPL variants that lead to increased plasma TG concentrations  
185 were linked to an increased risk of AAA.<sup>6</sup> The MR analysis also identified circulating LPL  
186 levels to be negatively associated with AAA risk (Fig 1B). To validate whether increased  
187 TG concentrations caused by impaired LPL activity can result in AAA development and  
188 rupture, we infused AngII into male, inducible *Lpl*-deficient (*iLpl<sup>f/f</sup>*) mice fed a low-  
189 cholesterol Western diet. With AngII infusion, an aortic rupture occurred in 94% (16/17,  
190 combined data from two cohorts of animal studies) of *iLpl<sup>f/f</sup>* mice compared to 9.5%  
191 (2/21, combined data from two cohorts of animal studies) aortic rupture rate in littermate  
192 control mice (Fig 2A-C, Supplementary Fig 1). The only survival *iLpl<sup>f/f</sup>* mouse did not  
193 have AAA and had a plasma TG concentration of 474 mg/dL and TC concentration of  
194 233 mg/dL. In contrast, after 1 week of Western diet feeding but before AngII infusion,  
195 the majority of the *iLpl<sup>f/f</sup>* mice had severely increased TG concentrations, which were as  
196 high as 11,103 mg/dL (4,077 ± 3,218 mg/dL) compared to 66 ± 28 mg/dL in *Lpl<sup>f/f</sup>* mice  
197 (Supplementary Fig 1A). Saline infusion, as a control, did not cause aortic rupture in  
198 either genotype (Supplementary Fig 1C). These findings showed that severely  
199 increased TG concentrations as a consequence of LPL deficiency resulted in aortic  
200 rupture and death in the AngII-induced AAA model.

201

202 Then, we employed other mouse strains with increased, but not severely elevated, TG  
203 concentrations to validate our hypothesis. We performed all the following AAA studies in  
204 mice fed a standard rodent laboratory diet to minimize the effects of  
205 hypercholesterolemia induced by a Western diet. ApoA-V is produced in the liver and  
206 secreted into circulation, where it exerts an important role in regulating plasma TG  
207 concentrations by enhancing LPL activity to hydrolyze triglycerides. Male *ApoA5*-  
208 deficient mice showed a 2-3-fold increase in TG concentrations but no difference in TC  
209 concentrations (Fig 2D-G), consistent with previous findings.<sup>12</sup> AAA was evaluated after  
210 a 4-week AngII infusion. The hypertriglyceridemic *ApoA5*-deficient mice had increased

211 AAA incidence and larger maximal abdominal aorta diameter (Fig 2E, H, I). There was  
212 no difference in blood pressure before and after AngII infusion between *Apoa5*-deficient  
213 mice and their littermate controls (Fig 2J). This phenotype was not observed in *Apoa5*-  
214 deficient female mice, which had only slightly increased TG concentrations (Fig 2K-O).  
215 In addition, female mice demonstrate markedly lower incidences of AAA than males due  
216 to sex hormones or sex chromosomes.<sup>26</sup> These findings imply the causative roles of  
217 elevated TG concentrations in AAA pathogenesis.

218

### 219 **Moderately to severely increased triglyceride levels accelerate AAA development** 220 **and rupture in human *APOC3* transgenic mice.**

221 Increased plasma ApoC-III concentrations are linked to enhanced production and  
222 slowed clearance of triglyceride-rich lipoproteins, causing hypertriglyceridemia. Human  
223 *APOC3* transgenic (h*APOC3* Tg) mice and age/sex-matched wild-type littermates were  
224 fed a standard rodent laboratory diet (Fig 3A). Compared with controls, male h*APOC3*  
225 Tg mice had about 7-fold increase in plasma TG concentrations (Fig 3B) and about 1-  
226 fold elevations in plasma TC concentrations (Fig 3C) and non-esterified fatty acids  
227 (NEFA, Fig 3D). We observed a low incidence of AAA in wild-type littermates (2 out of  
228 17), similar to the literature.<sup>26</sup> However, there was a dramatically increased AAA  
229 incidence and a larger maximal diameter of the suprarenal aorta in h*APOC3* Tg mice  
230 (11 out of 13 surviving animals), as well as a higher dissection rate (8 out of 13 surviving  
231 animals) and another 2 mice dying from AAA rupture (Fig 3E-H). There was no  
232 difference in systolic blood pressure (SBP) between h*APOC3* Tg mice and controls (Fig  
233 3I). A similar phenotype was observed in female mice (Fig 3J-O), indicating that  
234 dramatically increased TG concentrations accelerated AAA development, surpassing  
235 the protective effects of female hormones.

236

237 The effects of increased TG concentrations on AAA development were also evaluated in  
238 a PPE (porcine pancreatic elastase)-induced AAA model, in which AAA progression is  
239 independent of hypercholesterolemia.<sup>27</sup> Based upon a 50% increase in the maximal  
240 abdominal aorta diameter as AAA on day 14 post-operative, the incidence of AAA was  
241 100% for both male and female h*APOC3* Tg and littermate control mice (Supplementary  
242 Fig 2 and Supplementary Fig 3). Male h*APOC3* Tg mice showed significantly larger  
243 maximal aortic diameters than littermate controls, demonstrating that increased TG  
244 concentrations accelerated AAA growth (Supplementary Fig 2A-E). Even though female  
245 h*APOC3* Tg mice had lower TG concentrations than males (635 ± 36 mg/dL v.s. 946 ±  
246 258 mg/dL,  $p = 0.0005$ ), the increased TG concentrations in females were sufficient to  
247 cause larger aortic diameters (Supplementary Fig 3A-D).

248



249 These findings from the three hyperglyceridemia mouse models indicate that increased  
250 TG concentrations accelerate AAA rupture and aneurysm growth.

251

252 **Palmitate and increased triglyceride concentrations inhibit lysyl oxidase**  
253 **maturation in human aortic smooth muscle cells and aortas.**

254 The pathophysiology of AAA is intricately linked to the disruption of smooth muscle cell  
255 (SMC) homeostasis within the aortic wall, including phenotypic switching, cell death,  
256 extracellular matrix (ECM) remodeling, and inflammatory responses.<sup>28</sup> Serum from  
257 *Apoa5*-deficient or *hAPOC3* Tg mice, as well as VLDL and HDL particles, did not affect  
258 primary human aortic smooth muscle cell (HASMC) viability (Supplementary Fig 4A-C),  
259 while incubation with LDL slightly increased cell numbers (Supplementary Fig 4C). The  
260 presence of APOA5 in the conditional medium did not regulate the expression of  
261 contractile markers in the presence of either Platelet-Derived Growth Factor-BB (PDGF-  
262 BB) or Transforming growth factor-beta (TGF $\beta$ ) (data not shown), suggesting other  
263 mechanisms may exist. APOC3 overexpression caused elevated plasma TG  
264 concentrations accompanied by increased plasma NEFA concentrations (Fig 3D and  
265 Supplementary Fig 2C). Palmitic acid (PA) is the most common saturated fatty acid in  
266 the human body, typically accounting for 20–30% of the total fatty acids.<sup>29</sup> Bulk RNA  
267 sequencing (RNA-seq) analysis was performed to compare PA-incubated HASMC with  
268 BSA-treated (vehicle control) cells. Compared to the BSA-incubated group, PA-  
269 incubated HASMC showed an apparent reduction in ECM assembly pathways,  
270 including collagen chain trimerization, elastic fiber formation and maturation, (Fig 4A-D),  
271 and increased expression of the inflammation-related gene (Supplementary Fig 5A-B,  
272 Supplementary Table 4).

273

274 TGF- $\beta$  and lysyl oxidase (LOX) are crucial in regulating the cross-linking of collagen and  
275 elastin in the ECM. LOX was unexpectedly upregulated compared to the most  
276 downregulated genes in the elastic fiber formation and maturation pathways (Fig 4D). In  
277 primary HASMC, PA incubation induced the transcription of LOX, showing increased  
278 mRNA abundance by qRT-PCR (Fig 4E). LOX is initially synthesized as a preproprotein,  
279 which undergoes several post-translational modifications for its maturation and  
280 functional activation. Impairments in LOX activity, whether due to genetic mutations or  
281 LOX inhibitors, can lead to AAA formation and rupture.<sup>30-32</sup> Our RNA-seq data indicated  
282 that PA incubation downregulated the expression of BMP-1 (Bone morphogenetic  
283 protein 1), ADAMTS2 (a disintegrin and metalloproteinase with thrombospondin motif 2),  
284 and ADAMTS14, which are critical enzymes controlling LOX activation by the proteolytic  
285 removal of the propeptide region. We further confirmed that PA incubation  
286 downregulated BMP-1 and ADAMTS2 transcriptions in HASMCs (Fig 4F). Immunoblot  
287 analyses demonstrated that incubation with TGF- $\beta$  increased the abundance of the

288 mature form of LOX. However, the presence of PA blocked its effect, resulting in a less  
289 mature LOX (Fig 4G, I). LOX overexpression increased the mature form of LOX in  
290 HASMC, which was suppressed by incubation with PA (Fig 4H), indicating that PA  
291 interferes with the maturation process of LOX in HASMC. Nicotine, one of the well-  
292 established AAA risk factors, also repressed LOX maturation in HASMC  
293 (Supplementary Fig 6). These findings suggest that PA and nicotine may play a  
294 synergistic role in the pathogenesis of AAA by blocking LOX activation.

295  
296 To investigate the effects of increased circulating palmitate concentrations on the  
297 maturation of LOX in aortas, we administered ethyl palmitate, which can be hydrolyzed  
298 to free palmitate in rodents.<sup>33</sup> The mature LOX abundance in suprarenal abdominal  
299 aortas was inhibited significantly after administration of ethyl palmitate compared to the  
300 vehicle or control intact aortas (Fig 4J). Then, we examined whether increased TG  
301 concentrations affected the maturation of LOX in the aortas of hAPOC3 Tg and  
302 littermate control mice. There was no difference in the abundance of matured LOX in  
303 suprarenal abdominal aortas between the two groups without AngII infusion (Fig 4K).  
304 We observed a dramatic upregulation of mature LOX upon AngII infusion in control mice  
305 (Fig 4K), suggesting a protective and compensatory mechanism to enhance elastic fiber  
306 assembly to protect against the effects of AngII. However, this response disappeared in  
307 hAPOC3 Tg mice (Fig 4K), indicating that increased TG and/or palmitate inhibited LOX  
308 maturation in the aortas, which may contribute to AAA development and rupture.

### 309 310 ***Angptl3* ASO inhibits AAA formation and rupture in *APOC3* Tg mice.**

311 Based on the above findings, we asked whether lowering TG levels could attenuate  
312 AAA formation and rupture. We administered fenofibrate and niacin, commonly used for  
313 treating hypertriglyceridemia, but only observed a 14-17 % reduction of plasma TG  
314 concentrations in hAPOC3 Tg mice (Supplementary Fig 7). N-acetylgalactosamine  
315 (GalNAc)-conjugated antisense nucleotides (ASO) targeting of hepatocyte ANGPTL3  
316 results in significantly decreased plasma TG concentrations in animals and  
317 humans.<sup>15,16,34</sup> In hAPOC3 Tg mice, administration of *Angptl3* ASO dramatically  
318 suppressed hepatic *Angptl3* mRNA abundance by 64% and the plasma ANGPTL3  
319 concentrations by 81% (Fig 5A-C). Consequently, administration of the *Angptl3* ASO  
320 significantly reduced concentrations of NEFA, triglycerides (from 1,119 ± 98 mg/dL to  
321 586 ± 114 mg/dL) and total cholesterol (from 283 ± 103 mg/dL to 117 ± 58 mg/dL) (Fig  
322 5D-F). Consistent with the above findings, increased TG concentrations in hAPOC3 Tg  
323 mice accelerated AAA development during AngII infusion (Fig 5G-L). After  
324 administration of *Angptl3* ASO to hAPOC3 Tg mice, we recorded significant reductions  
325 in AAA incidence, maximal aortic diameter, elastin degradation, and dissection,  
326 comparable to the control mice (Fig 5G-L). qRT-PCR and ELISA analysis showed no

327 significant changes in the levels of mouse *Apoc3* and human *APOC3* (Fig 5M-P). There  
328 were no significant changes in the TG and TC metabolism-related genes in the liver,  
329 such as *Apoc2*, *Apoa5*, *ApoE*, *Apob*, *Mttp*, *Fasn*, *Srebp1c*, *Ldlr*, and *Pcsk9*  
330 (Supplementary Fig 8). *Angptl3* ASO administration did not significantly change body  
331 weight or systolic blood pressure (Fig 5Q-R). Overall, our findings demonstrate that  
332 administration of *Angptl3* ASO protected against hypertriglyceridemia accelerated AAA  
333 development in hAPOC3 Tg mice.

334

### 335 ***Angptl3* ASO inhibits AAA development in *ApoE*-deficient mice.**

336 ApoE-deficient mice have high levels of VLDL due to impaired clearance of chylomicron  
337 and VLDL. Compared with age and sex-matched C57BL/6J mice, *ApoE*-deficient mice  
338 show significantly increased plasma levels of TC and moderately increased TG levels  
339 when fed a standard rodent diet.<sup>35</sup> Similar to the observation in hAPOC3 Tg mice,  
340 administration of *Angptl3* ASO dramatically reduced hepatic *Angptl3* mRNA expression  
341 and the circulating levels of ANGPTL3 (Fig 6A-C). As expected, administration of the  
342 *Angptl3* ASO significantly decreased TG concentrations by 50%, NEFA by 31%, and  
343 slightly decreased TC concentrations by 8% in *ApoE*-deficient mice fed a standard  
344 rodent laboratory diet (Fig 6D-F). We also used size exclusion chromatography to  
345 separate lipoprotein classes and found decreased TG concentrations, mainly in VLDL  
346 and IDL (Fig 6I), while cholesterol concentrations were slightly reduced in VLDL and  
347 HDL (Fig 6J). Blood pressure measurements and body weight recordings revealed no  
348 significant difference between control ASO and *Angptl3* ASO-administered mice (Fig  
349 6G, H). Consistent with the literature, AAA incidence in *ApoE*-deficient mice was 83% in  
350 the control group (Fig 6K, N). *Angptl3* ASO administration largely inhibited AAA  
351 development, as evidenced by significantly decreased AAA incidence and maximal  
352 aortic diameters (Fig 6N, O). Depletion of hepatic *Angptl3* had limited effects on the  
353 expression of genes involved in lipogenesis and cholesterol metabolism (Fig 6P). Taken  
354 together, these data demonstrated that lowering TG and NEFA concentrations by  
355 *Angptl3* ASO inhibited AAA development in *ApoE*-deficient mice.

356

## 357 **Discussion**

358 AAA screening programs have identified many asymptomatic AAA and effectively  
359 reduced aneurysm-related mortality. Thus, limiting aneurysm growth and reducing the  
360 risk of aneurysm rupture has become a key priority for the treatment of AAA.<sup>36</sup> Based on  
361 the genetic, proteomic, and metabolomic findings, we identify that increased TG  
362 concentrations accelerate AAA formation and rupture using three hypertriglyceridemia  
363 murine models. Of clinical relevance, we provide evidence that lowering TG and NEFA

364 concentrations by *Angptl3* ASO administration dramatically inhibited AAA development  
365 and rupture.

366  
367 Mendelian Randomization (MR) using protein quantitative trait loci (pQTLs) as  
368 instrumental variables (IVs) can help infer causality and identify drug targets for  
369 complex diseases. By integrating pQTLs from ten large GWAS on circulating proteins,  
370 we updated the 'actionable' druggable target pool into an enlarged set of 2,698 proteins.  
371 Genetically determined APOA5 and LPL, two critical molecules regulating triglyceride  
372 metabolism, were negatively associated with AAA risk. In contrast, the variants related  
373 to APOC3 with increased TG concentrations were associated with increased AAA risk,  
374 underscoring the role of triglyceride metabolism in human AAA development, consistent  
375 with other genetic findings.<sup>7,8</sup> We further explored the causal effects of metabolites on  
376 AAA risk using IVs from 233 NMR-measured circulating metabolites.<sup>20</sup> The strong  
377 associations found in VLDL and its subfractions as well as free fatty acid concentrations,  
378 further highlighted the importance of TG metabolism in AAA. Collectively, these findings  
379 emphasize the significance of TG in AAA risk and provide potential candidates for AAA  
380 prevention and treatment.

381  
382 According to the literature and our experience, young C57BL/6J mice, when fed a  
383 standard rodent laboratory diet, have low AAA incidence when infused with AngII.<sup>26,37</sup>  
384 Hyperlipidemia increases the AAA incidence during AngII infusion in *Ldlr* and *ApoE*-  
385 deficient mice or C57BL/6J mice with an AAV expressing a gain-of-function mutant of  
386 PCSK9, in which *Ldlr*-deficient mice and PCSK9 overexpressing mice are fed a Western  
387 diet to augment hypercholesterolemia.<sup>26</sup> Compared with C57BL/6J mice, *Ldlr* or *ApoE*-  
388 deficient mice have significantly increased TC and TG concentrations, which mainly  
389 distribute in VLDL fractions using size exclusion chromatography to separate lipoprotein  
390 classes,<sup>38</sup> indicating that increased concentrations of large, TG-rich lipoproteins are  
391 associated with AAA formation. Our previous study demonstrated that AAA development  
392 is accelerated with modestly hypercholesterolemic conditions, but further elevation of  
393 cholesterol above a threshold level does not enhance AAA progression.<sup>37</sup> Here, we  
394 present that increased TG concentrations contribute to AAA development, dissection,  
395 and rupture in a TG-concentration-dependent manner using three hypertriglyceridemia  
396 mouse models. The moderately increased TG concentrations in *Apoa5* deficiency mice  
397 accelerated AAA development, dramatically increased TG concentrations in hAPOC3  
398 transgenic mice caused AAA dissection, and severely high TG concentrations resulted  
399 in aortic rupture and death in inducible *Lpl*-deficient mice. We also evaluated the effects  
400 of increased TG concentrations on aneurysm growth in the elastase-induced AAA  
401 model. Previous studies have demonstrated that the aneurysm growth in the PPE  
402 model is independent of hypercholesterolemic conditions using C57BL/6J mice with

403 PCSK9 overexpression or *ApoE*-deficient mice.<sup>27,39</sup> Using the PPE-induced AAA model,  
404 we demonstrated that increased TG concentrations aggravated AAA growth in both  
405 male and female *APOC3* Tg mice. Furthermore, clinical observation shows that plasma  
406 TG concentrations are higher in AAA patients than in controls.<sup>9</sup> In a prospective  
407 epidemiological study (the British United Provident Association [BUPA] study), the risk of  
408 death from AAA rupture is strongly related to serum TG concentrations.<sup>10</sup> Together,  
409 these findings pave the way for future studies of the role of triglyceride and related  
410 metabolites in AAA development.

411  
412 Importantly, our study demonstrates that lowering TG and NEFA levels by administrating  
413 *Angptl3* ASO inhibits AAA development in both h*APOC3* transgenic mice and *ApoE*-  
414 deficient mice. ApoC-III raises TG concentrations by inhibiting LPL activity, reducing  
415 hepatic uptake of TG-rich lipoproteins, and promoting VLDL secretion. ApoE acts as a  
416 critical ligand for the LDL receptor and the LDL receptor-related protein, facilitating the  
417 uptake of chylomicron and VLDL remnants into hepatocytes. Deficiency of ApoE causes  
418 elevated TG and TC levels. In both *APOC3* transgenic mice and *ApoE*-deficient mice,  
419 triglycerides and cholesterol are mainly distributed in VLDL fractions. Administration of  
420 *Angptl3* ASO dramatically reduced TG levels in VLDL and IDL fractions, consistent with  
421 decreased TG concentrations in plasma, supporting the hypothesis that large-sized TG-  
422 rich lipoproteins and related metabolites contribute to AAA progression and rupture.  
423 These findings also provide evidence that lowering TG-rich lipoproteins is a potential  
424 therapeutic strategy. ANGPTL8 and ANGPTL3 form a complex that markedly inhibits  
425 LPL activity. Similar to the effects of *Angptl3* ASO on AAA, *Angptl8*-deficiency or  
426 knockdown reduced AAA formation by lowering TG concentrations and suppressing the  
427 inflammatory response in *ApoE*-deficient mice.<sup>40</sup> Administration of fenofibrate also  
428 reduced the severity of experimental AAA in *Ldlr*- and *ApoE*-deficient mice.<sup>41,42</sup>  
429 However, fenofibrate did not significantly limit AAA growth in AAA patients in FAME-2  
430 (Fenofibrate in the Management of Abdominal Aortic Aneurysm 2), a placebo-controlled  
431 clinical trial.<sup>43</sup> We should note that it may take an estimated five years for a small AAA  
432 with a diameter of 40–55 mm to reach 55 mm, the size threshold for intervention.<sup>36</sup> In  
433 the FAME-2 study, AAA diameters in the control group increased only about 1 mm after  
434 a 24-week observation period, making it hard to determine the effects of fenofibrate.  
435 Additionally, AAA diameters in the two groups began to diverge at the end of the  
436 evaluation, suggesting that a long-term clinical trial with a larger sample size is needed  
437 to carefully assess the effects of triglyceride-lowering on AAA growth and rupture.

438  
439 AAA is characterized by pathological remodeling of the aortic ECM, including elastolysis  
440 and collagenolysis. LOX is a crucial enzyme involved in the cross-linking of collagen  
441 and elastin in the ECM to maintain the structural integrity of the aortic wall. Impairments

442 in LOX activity due to genetic mutations can lead to connective tissue disorders and  
443 promote aorta dissection.<sup>44</sup> *Lox*-deficient mice exhibit severe defects in vascular  
444 development, leading to perinatal death from aortic aneurysm.<sup>31</sup>  $\beta$ -Aminopropionitrile  
445 (BAPN) is a well-known inhibitor of LOX and has been used extensively in research to  
446 accelerate AAA formation and rupture.<sup>45</sup> LOX is initially synthesized as a preproprotein  
447 and secreted into the extracellular space, where the prolysinase is cleaved by  
448 proteases, including BMP-1, ADAMTS-2, and ADAMTS-14. Increased TG  
449 concentrations or the presence of palmitate dramatically blocked LOX maturation in  
450 aortas and HASMCs. Based on RNA-seq findings, BMP-1 and ADAMTS-2 are highly  
451 abundant in HASMC. PA downregulated the expression of BMP-1 and ADAMTS-2,  
452 causing decreased LOX maturation. Additionally, PA induces vascular SMC apoptosis,  
453 promotes inflammatory responses, enhances oxidative stress, and triggers proliferation  
454 and migration, contributing to the progression of vascular diseases such as  
455 atherosclerosis and hypertension.<sup>46</sup> In this study, we demonstrated that PA, potentially  
456 originating from plasma triglycerides, may contribute to AAA development by inhibiting  
457 LOX maturation. Lowering TG and NEFA by administration of *Angptl3* ASO can inhibit  
458 AAA development, suggesting that managing triglyceride concentrations and related  
459 metabolites through lifestyle changes and pharmacotherapy may reduce the risk of AAA  
460 development.

461  
462 Plasma TG concentrations include the content of various lipoprotein particles. Multiple  
463 genes, such as LPL, APOC3, APOC2, APOA5, and ANGPTL3, influence TG  
464 metabolism and regulate plasma TG concentrations. Among them, APOC3 and  
465 ANGPTL3 are targets for drug development because loss-of-function mutations in  
466 APOC3 and ANGPTL3 are associated with improved lipid profiles and reduced  
467 cardiovascular risk. Preclinical and clinical data have well documented that ApoC-III or  
468 ANGPTL3 inhibitors effectively reduce severe hypertriglyceridemia. These inhibitors  
469 include antisense nucleotides (ASO),<sup>14,16,34</sup> monoclonal antibodies (mAb),<sup>47</sup> small  
470 interfering RNA (siRNA),<sup>48,49</sup> and CRISPR-cas gene editing strategies.<sup>50,51</sup> Preclinical  
471 and clinical data have demonstrated that ANGPTL3 inhibitors are highly effective for  
472 treating severe hypertriglyceridemia by upregulating LPL activity and facilitating the  
473 hydrolysis and clearance of TG-rich lipoproteins. As hAPOC3 transgenic mice have very  
474 high APOC3 and TG concentrations, *Angptl3* ASO was administered at 50 mg/kg/week  
475 in previous studies.<sup>16</sup> In this study, administration of an *Angptl3* ASO at a much lower  
476 dosage effectively reduced AAA development in hAPOC3 transgenic mice and *ApoE*-  
477 deficient mice through reducing TG concentrations, especially TG concentrations in  
478 VLDL fractions. We observed that the administration of *Angptl3* ASO mainly decreased  
479 plasma TG concentrations with a limited reduction in plasma TC concentrations, further

480 supporting the idea that managing TG-rich lipoprotein concentrations is a potential  
481 therapeutic strategy for treating AAA.

482

483 In summary, the present studies, combined with recent genetic, proteomic, and  
484 metabolomic findings, indicate that increased TG concentrations increase AAA risk.  
485 Individuals at higher genetic risk for AAA might benefit from targeted interventions.  
486 Understanding the association between triglyceride concentrations and AAA risk has  
487 important clinical implications. These findings prove that ASO administration targeting  
488 ANGPTL3 may become a therapy to reduce the risk of AAA. The present studies should  
489 stimulate further experimental and clinical investigations of the mechanisms and  
490 therapeutic strategies for AAA treatment via triglyceride-lowering therapies.

491 **Funding**

492 This study was partially supported by the National Institutes of Health grants HL166203  
493 (Y.G.), HL165688 (Y.G. and A.S.), HL109946 and HL134569 (Y.E.C.), HL151524 (L.C.),  
494 HL153710 and HL138139 (J.Z.), HL172832 (G. Zhao), R35HL155649 (A.D.),  
495 UL1TR001998 (A.D.), R21 NS11191 (A.S.) and the American Heart Association Merit  
496 award 23MERIT1036341 (A.D.).

497

498 **Disclosures**

499 The authors have no competing interests.

500

501 **Data availability**

502 All genetic data used in this study were obtained from publicly available consortiums.  
503 The RNAseq original data generated during this study will be deposited in a publicly  
504 accessible database upon acceptance of the manuscript.



## 505 References

- 506 1. Nordon, I.M., Hinchliffe, R.J., Loftus, I.M. & Thompson, M.M. Pathophysiology  
507 and epidemiology of abdominal aortic aneurysms. *Nat Rev Cardiol* **8**, 92-102  
508 (2011).
- 509 2. United Kingdom Small Aneurysm Trial, P., *et al.* Long-term outcomes of  
510 immediate repair compared with surveillance of small abdominal aortic  
511 aneurysms. *N Engl J Med* **346**, 1445-1452 (2002).
- 512 3. Soden, P.A., *et al.* Outcomes for symptomatic abdominal aortic aneurysms in the  
513 American College of Surgeons National Surgical Quality Improvement Program.  
514 *J Vasc Surg* **64**, 297-305 (2016).
- 515 4. Reimerink, J.J., van der Laan, M.J., Koelemay, M.J., Balm, R. & Legemate, D.A.  
516 Systematic review and meta-analysis of population-based mortality from ruptured  
517 abdominal aortic aneurysm. *Br J Surg* **100**, 1405-1413 (2013).
- 518 5. Golledge, J., Thanigaimani, S., Powell, J.T. & Tsao, P.S. Pathogenesis and  
519 management of abdominal aortic aneurysm. *Eur Heart J* **44**, 2682-2697 (2023).
- 520 6. Roychowdhury, T., *et al.* Genome-wide association meta-analysis identifies risk  
521 loci for abdominal aortic aneurysm and highlights PCSK9 as a therapeutic target.  
522 *Nat Genet* **55**, 1831-1842 (2023).
- 523 7. Harrison, S.C., *et al.* Genetic Association of Lipids and Lipid Drug Targets With  
524 Abdominal Aortic Aneurysm: A Meta-analysis. *JAMA Cardiol* **3**, 26-33 (2018).
- 525 8. Klarin, D., *et al.* Genetics of blood lipids among ~300,000 multi-ethnic  
526 participants of the Million Veteran Program. *Nat Genet* **50**, 1514-1523 (2018).
- 527 9. Norrgard, O., Angquist, K.A. & Johnson, O. Familial aortic aneurysms: serum  
528 concentrations of triglyceride, cholesterol, HDL-cholesterol and (VLDL + LDL)-  
529 cholesterol. *Br J Surg* **72**, 113-116 (1985).
- 530 10. Watt, H.C., *et al.* Serum triglyceride: a possible risk factor for ruptured abdominal  
531 aortic aneurysm. *Int J Epidemiol* **27**, 949-952 (1998).
- 532 11. Subramanian, S. Hypertriglyceridemia: Pathophysiology, Role of Genetics,  
533 Consequences, and Treatment. in *Endotext* (eds. Feingold, K.R., *et al.*) (South  
534 Dartmouth (MA), 2000).
- 535 12. Pennacchio, L.A., *et al.* An apolipoprotein influencing triglycerides in humans and  
536 mice revealed by comparative sequencing. *Science* **294**, 169-173 (2001).
- 537 13. Breckenridge, W.C., Little, J.A., Steiner, G., Chow, A. & Poapst, M.  
538 Hypertriglyceridemia associated with deficiency of apolipoprotein C-II. *N Engl J*  
539 *Med* **298**, 1265-1273 (1978).
- 540 14. Witztum, J.L., *et al.* Volanesorsen and Triglyceride Levels in Familial  
541 Chylomicronemia Syndrome. *N Engl J Med* **381**, 531-542 (2019).

- 542 15. Bergmark, B.A., *et al.* Olezarsen for Hypertriglyceridemia in Patients at High  
543 Cardiovascular Risk. *N Engl J Med* **390**, 1770-1780 (2024).
- 544 16. Graham, M.J., *et al.* Cardiovascular and Metabolic Effects of ANGPTL3  
545 Antisense Oligonucleotides. *N Engl J Med* **377**, 222-232 (2017).
- 546 17. Rosenson, R.S., *et al.* Zodasiran, an RNAi Therapeutic Targeting ANGPTL3, for  
547 Mixed Hyperlipidemia. *N Engl J Med* (2024).
- 548 18. Burgess, S., *et al.* Using genetic association data to guide drug discovery and  
549 development: Review of methods and applications. *Am J Hum Genet* **110**, 195-  
550 214 (2023).
- 551 19. Gaziano, L., *et al.* Actionable druggable genome-wide Mendelian randomization  
552 identifies repurposing opportunities for COVID-19. *Nat Med* **27**, 668-676 (2021).
- 553 20. Karjalainen, M.K., *et al.* Genome-wide characterization of circulating metabolic  
554 biomarkers. *Nature* **628**, 130-138 (2024).
- 555 21. Ibrahim, M., Thanigaimani, S., Singh, T.P., Morris, D. & Golledge, J. Systematic  
556 review and Meta-Analysis of Mendelian randomisation analyses of Abdominal  
557 aortic aneurysms. *Int J Cardiol Heart Vasc* **35**, 100836 (2021).
- 558 22. Raffort, J., *et al.* Diabetes and aortic aneurysm: current state of the art.  
559 *Cardiovasc Res* **114**, 1702-1713 (2018).
- 560 23. Daugherty, A. & Cassis, L. Chronic angiotensin II infusion promotes  
561 atherogenesis in low density lipoprotein receptor *-/-* mice. *Ann N Y Acad Sci* **892**,  
562 108-118 (1999).
- 563 24. Daugherty, A., Manning, M.W. & Cassis, L.A. Angiotensin II promotes  
564 atherosclerotic lesions and aneurysms in apolipoprotein E-deficient mice. *J Clin*  
565 *Invest* **105**, 1605-1612 (2000).
- 566 25. Lu, H., *et al.* Hypercholesterolemia Induced by a PCSK9 Gain-of-Function  
567 Mutation Augments Angiotensin II-Induced Abdominal Aortic Aneurysms in  
568 C57BL/6 Mice-Brief Report. *Arterioscler Thromb Vasc Biol* **36**, 1753-1757 (2016).
- 569 26. Sawada, H., Lu, H.S., Cassis, L.A. & Daugherty, A. Twenty Years of Studying  
570 AngII (Angiotensin II)-Induced Abdominal Aortic Pathologies in Mice: Continuing  
571 Questions and Challenges to Provide Insight Into the Human Disease.  
572 *Arterioscler Thromb Vasc Biol* **42**, 277-288 (2022).
- 573 27. Mulorz, J., *et al.* Hyperlipidemia does not affect development of elastase-induced  
574 abdominal aortic aneurysm in mice. *Atherosclerosis* **311**, 73-83 (2020).
- 575 28. Golledge, J. Abdominal aortic aneurysm: update on pathogenesis and medical  
576 treatments. *Nat Rev Cardiol* **16**, 225-242 (2019).
- 577 29. Carta, G., Murru, E., Banni, S. & Manca, C. Palmitic Acid: Physiological Role,  
578 Metabolism and Nutritional Implications. *Front Physiol* **8**, 902 (2017).
- 579 30. Staiculescu, M.C., Kim, J., Mecham, R.P. & Wagenseil, J.E. Mechanical behavior  
580 and matrix gene expression in the aneurysm-prone thoracic aorta of

- 581 newborn lysyl oxidase knockout mice. *Am J Physiol Heart Circ Physiol* **313**,  
582 H446-H456 (2017).
- 583 31. Lee, V.S., *et al.* Loss of function mutation in LOX causes thoracic aortic  
584 aneurysm and dissection in humans. *Proc Natl Acad Sci U S A* **113**, 8759-8764  
585 (2016).
- 586 32. Franklin, M.K., *et al.* beta-Aminopropionitrile Induces Distinct Pathologies in the  
587 Ascending and Descending Thoracic Aortic Regions of Mice. *Arterioscler Thromb*  
588 *Vasc Biol* **44**, 1555-1569 (2024).
- 589 33. Eguchi, K., *et al.* Saturated fatty acid and TLR signaling link beta cell dysfunction  
590 and islet inflammation. *Cell Metab* **15**, 518-533 (2012).
- 591 34. Bergmark, B.A., *et al.* Effect of Vupanorsen on Non-High-Density Lipoprotein  
592 Cholesterol Levels in Statin-Treated Patients With Elevated Cholesterol:  
593 TRANSLATE-TIMI 70. *Circulation* **145**, 1377-1386 (2022).
- 594 35. Plump, A.S., *et al.* Severe hypercholesterolemia and atherosclerosis in  
595 apolipoprotein E-deficient mice created by homologous recombination in ES  
596 cells. *Cell* **71**, 343-353 (1992).
- 597 36. Ulug, P., Powell, J.T., Martinez, M.A., Ballard, D.J. & Filardo, G. Surgery for small  
598 asymptomatic abdominal aortic aneurysms. *Cochrane Database Syst Rev* **7**,  
599 CD001835 (2020).
- 600 37. Liu, J., *et al.* Associations of ApoA1 and ApoB-containing lipoproteins with AngII-  
601 induced abdominal aortic aneurysms in mice. *Arterioscler Thromb Vasc Biol* **35**,  
602 1826-1834 (2015).
- 603 38. Ishibashi, S., Herz, J., Maeda, N., Goldstein, J.L. & Brown, M.S. The two-  
604 receptor model of lipoprotein clearance: tests of the hypothesis in "knockout"  
605 mice lacking the low density lipoprotein receptor, apolipoprotein E, or both  
606 proteins. *Proc Natl Acad Sci U S A* **91**, 4431-4435 (1994).
- 607 39. Ikezoe, T., *et al.* No Effect of Hypercholesterolemia on Elastase-Induced  
608 Experimental Abdominal Aortic Aneurysm Progression. *Biomolecules* **11**(2021).
- 609 40. Yu, H., *et al.* ANGPTL8 deletion attenuates abdominal aortic aneurysm formation  
610 in ApoE<sup>-/-</sup> mice. *Clin Sci (Lond)* **137**, 979-993 (2023).
- 611 41. Krishna, S.M., *et al.* Fenofibrate increases high-density lipoprotein and  
612 sphingosine 1 phosphate concentrations limiting abdominal aortic aneurysm  
613 progression in a mouse model. *Am J Pathol* **181**, 706-718 (2012).
- 614 42. Golledge, J., *et al.* Peroxisome proliferator-activated receptor ligands reduce  
615 aortic dilatation in a mouse model of aortic aneurysm. *Atherosclerosis* **210**, 51-56  
616 (2010).
- 617 43. Pinchbeck, J.L., *et al.* Randomized Placebo-Controlled Trial Assessing the Effect  
618 of 24-Week Fenofibrate Therapy on Circulating Markers of Abdominal Aortic

- 619           Aneurysm: Outcomes From the FAME -2 Trial. *J Am Heart Assoc* **7**, e009866  
620           (2018).
- 621   44.    Guo, D.C., *et al.* LOX Mutations Predispose to Thoracic Aortic Aneurysms and  
622           Dissections. *Circ Res* **118**, 928-934 (2016).
- 623   45.    Kanematsu, Y., *et al.* Pharmacologically induced thoracic and abdominal aortic  
624           aneurysms in mice. *Hypertension* **55**, 1267-1274 (2010).
- 625   46.    Hu, Y., Fan, Y., Zhang, C. & Wang, C. Palmitic acid inhibits vascular smooth  
626           muscle cell switch to synthetic phenotype via upregulation of miR-22 expression.  
627           *Aging (Albany NY)* **14**, 8046-8060 (2022).
- 628   47.    Gaudet, D., *et al.* Evinacumab in homozygous familial hypercholesterolaemia:  
629           long-term safety and efficacy. *Eur Heart J* **45**, 2422-2434 (2024).
- 630   48.    Watts, G.F., *et al.* RNA interference targeting ANGPTL3 for triglyceride and  
631           cholesterol lowering: phase 1 basket trial cohorts. *Nat Med* **29**, 2216-2223  
632           (2023).
- 633   49.    Gaudet, D., *et al.* RNA Interference Therapy Targeting Apolipoprotein C-III in  
634           Hypertriglyceridemia. *NEJM Evid* **2**, EVIDo2200325 (2023).
- 635   50.    Zha, Y., *et al.* CRISPR/Cas9-mediated knockout of APOC3 stabilizes plasma  
636           lipids and inhibits atherosclerosis in rabbits. *Lipids Health Dis* **20**, 180 (2021).
- 637   51.    Zuo, Y., *et al.* Liver-specific in vivo base editing of Angptl3 via AAV delivery  
638           efficiently lowers blood lipid levels in mice. *Cell Biosci* **13**, 109 (2023).
- 639

## 640 **Figures**

### 641 **Fig. 1: Mendelian Randomization identifies circulating proteins and metabolites** 642 **causally related to AAA risk.**

643 **A**, Outline of the analyses performed. Two-sample Mendelian Randomization (MR)  
644 analyses were applied to determine the causal effects of circulating proteins, and  
645 nuclear magnetic resonance (NMR) measured circulating metabolites on the risk of  
646 abdominal aortic aneurysm (AAA) using multiple data sources. **B**, Forest plot displaying  
647 the causal effects of 41 proteins identified through MR-Wald ratio analysis after  
648 Bonferroni correction. **C**, Classifications of NMR metabolites and the relative lipid  
649 compositions of the 14 lipoprotein subclasses (left). All 14 lipoprotein subclass particles  
650 are illustrated using the same size scale, with diameters based on mean values from  
651 5,651 participants in the Northern Finland Birth Cohort 1966 (NFBC66). Note that the  
652 size of the LDL and HDL particles in the figure is multiplied by 1.5 and 2.0, respectively.  
653 The right side features a circular histplot of the MR results for 141 metabolites. Each  
654 bar's height represents the absolute effect size, while the color indicates the direction  
655 and P-value as determined by the MR inverse-variance weighted (IVW) method.

656

### 657 **Fig. 2: Impaired LPL activity accelerates AAA development and aortic rupture.**

658 **A**, Design of the AAA study in *Lpl*-deficient mice. Inducible global *Lpl*-deficient mice  
659 were generated by crossing *Lpl* floxed (*Lpl*<sup>f/f</sup>) mice with  $\beta$ -actin driven tamoxifen-  
660 inducible MerCreMer transgenic mice. Low cholesterol, Western diet feeding was  
661 initiated 2 weeks after the start of tamoxifen treatment. **B**, Aortic rupture incidence curve  
662 during 4 weeks of AngII infusion. **C**, Aortic aneurysm incidence in *Lpl*<sup>f/f</sup> (n=11) and *iLpl*<sup>-/-</sup>  
663 (n=10) mice. **D**, Design of the AAA study in *Apoa5*-deficient mice. Mice were fed a  
664 standard rodent laboratory diet. After 4-week of AngII infusion, aortas from surviving  
665 mice were harvested. **E**, Representative aorta of male WT (n = 14) and *Apoa5*-deficient  
666 (n = 15) mice after 4 weeks of AngII infusion. Plasma samples were collected on day 28  
667 and subjected individually to analytical chemistry to measure triglycerides (TG) and total  
668 cholesterol (TC). **F-J**, The TG (**F**), TC (**G**), maximal aortic diameter (**H**), AAA incidence  
669 (**I**), and systolic blood pressure (**J**) in male mice. **K-O**, TG (**K**), TC (**L**), maximal aortic  
670 diameter (**M**), AAA incidence (**N**), and systolic blood pressure (**O**) in female WT (n = 10)  
671 and *Apoa5*-deficient (n = 8) mice in AngII-induced AAA study. Data are presented as  
672 circles and Mean  $\pm$  SEM (**F-H**, **J -M**, **O**). Statistical analyses were conducted as follows:  
673 Chi-Squared test for **C**, **I**, **N**; Mann-Whitney U test for **F**, **M**; Student's t-test for **G**, **H**, **K**,  
674 **L**; Kruskal-Wallis test followed by Dunn's post hoc analysis for **J**; One-way ANOVA  
675 followed by Sidak post hoc analysis for **O**. SBP, systolic blood pressure.

676 **Fig. 3: Dramatically increased TG concentrations accelerate AAA development**  
677 **and rupture in hAPOC3 Tg mice.**

678 **A**, Design of the AAA study in human *APOC3* transgenic (h*APOC3* Tg) mice. Twelve- to  
679 16-week-old h*APOC3* Tg mice (n of male = 15; n of female = 24) or WT littermates (n of  
680 male = 17, n of female = 21) were infused with AngII (1,000 ng/kg/min) for 4 weeks to  
681 induce AAA. Systolic blood pressures were measured before and after AngII infusion.  
682 The mice were fed a standard rodent laboratory diet. After 4 weeks, aortas from  
683 surviving mice were harvested. Plasma samples were collected on day 28 and  
684 subjected individually to analytical chemistry. **B-D**, plasma triglycerides (TG) (**B**), total  
685 cholesterol (TC) (**C**), and non-esterified fatty acids (**D**) in male mice. Representative  
686 aortas of male WT and h*APOC3* Tg mice after 4 weeks of AngII infusion (**E**). Maximal  
687 aortic diameter (**F**), AAA incidence (**G**), dissection rate (**H**), and systolic blood pressure  
688 (**I**) in male mice. **J-Q**, The TG (**J**), TC (**K**), non-esterified fatty acids (**L**), maximal aortic  
689 diameter (**M**), AAA incidence (**N**), and dissection rate (**O**) in female WT and h*APOC3* Tg  
690 mice after 4 weeks of AngII infusion. Data are presented as circles and Mean  $\pm$  SEM (**B**-  
691 **D**, **F**, **I-M**). Statistical analyses were conducted as follows: Mann-Whitney U test for **B**,  
692 **D**, **F**, **J**, **K**; Student's t-test for **C**, **L**, **M**; Chi-Squared test for **G**, **H**, **N**, **O**; One-way  
693 ANOVA followed by Sidak post hoc analysis for **I**. Scale bars: 1 mm in **E**. SBP, systolic  
694 blood pressure; NEFA, non-esterified fatty acids.

695

696 **Fig. 4: Palmitic acid inhibits LOX maturation in HASMCs and aortas.**

697 **A-F**, Human aortic smooth muscle cells (HASMCs) were starved in OptiMEM-reduced  
698 serum medium for 24 hours, followed by incubation with palmitic acid (250  $\mu$ M; PA) or  
699 vehicle (BSA) for another 24 hours. Total RNA was extracted for RNA sequencing or  
700 qRT-PCR. **A**, Reactome pathway enrichment analysis of down-regulated genes in the  
701 PA group. **B**, Top 5 downregulated Reactome pathways identified from Gene Set  
702 Enrichment Analysis (GSEA). **C**, Heatmap of gene expression levels in the collagen  
703 chain trimerization pathway. **D**, Heatmap of gene expression levels involved in elastic  
704 fiber formation and maturation. qRT-PCR analysis of *LOX* (**E**) and *BMP1*, *ADAMTS2*,  
705 and *ADAMTS14* (**F**) (data from 4 independent experiments). **G**, **I**, HASMCs were  
706 starved in OptiMEM for 24 hours, then incubated with PA (250  $\mu$ M) or vehicle along with  
707 TGF- $\beta$  (10 ng/ml) or vehicle for another 24 hours. Total proteins were extracted for  
708 Western blot analysis. **G**, Representative Western blot image of mature LOX and  
709 premature form of LOX. **I**, Quantification analysis of mature LOX protein abundance  
710 (data from 5 independent experiments). **H**, HASMCs were transfected with adenovirus  
711 LacZ or LOX (30 MOI) for 2 hours in a growth medium, then starved in OptiMEM for  
712 another 22 hours. Cells were incubated with PA (250  $\mu$ M) or vehicle for an additional 24

713 hours. Total proteins were then extracted for Western blot analysis of mature and  
714 premature LOX. **J**, Eight-week-old male C57BL/6J mice were given saline, vehicle, or  
715 ethyl palmitate (600 mg/kg) for 5 consecutive days via intraperitoneal injection. On day  
716 6, mice were euthanized, suprarenal abdominal aortas were isolated, and total protein  
717 was extracted and analyzed by Western blot to detect mature LOX abundance in  
718 suprarenal abdominal aortas, with corresponding quantifications (n = 5/group). **K**,  
719 Twelve- to 16-week-old hAPOC3 Tg mice and littermate control mice were infused with  
720 saline or AngII (1,000 ng/kg/min) for 7 days. On day 8, mice were euthanized,  
721 suprarenal abdominal aortas were isolated, and total protein was extracted and  
722 analyzed by Western blot to detect mature LOX expression in suprarenal abdominal  
723 aortas, with corresponding quantifications (n = 3 or 4/genotyping/treatment). Data are  
724 presented as dots and Mean  $\pm$  SEM (**E**, **F**, **I-K**). Statistical analyses were conducted as  
725 follows: Student's t-test for **E**, **F**; Mann-Whitney U test followed by Bonferroni correction  
726 for **I**; One-way ANOVA followed by Sidak post hoc analysis for **J**, **K**.

727

728 **Fig. 5: Administration of *Angptl3* ASO prevents AAA formation in hAPOC3 Tg**  
729 **mice.**

730 **A**, Design of the *Angptl3* ASO study in human APOC3 Tg mice. Twelve- to 16-week-old  
731 male hAPOC3 Tg mice were given one injection of *Angptl3* ASO (10 mg/kg) or  
732 scrambled ASO by subcutaneous administration. After 3 days, mice were infused with  
733 AngII (1,000 ng/kg/min) for 25 days. Three more injections (3 mg/kg) were conducted  
734 on days 7, 14, and 21. A wild-type group was included, receiving injections of scramble  
735 ASO. At the end of the study, aortas, livers, and plasma were harvested. **B**, Relative  
736 abundance of *Angptl3* mRNA in livers of the three groups. **C-D**, Plasma ANGPTL3  
737 protein concentrations (**C**) and non-esterified fatty acids (**D**) at the endpoint. **E to F**,  
738 Plasma triglycerides (TG) (**E**) and total cholesterol (TC) (**F**) concentrations on days 0, 3,  
739 and 28. **G**, Representative aortic trees from the 3 groups. **H**, Representative H&E  
740 staining (left) and Verhoeff-Van Gieson (VVG) staining (right) of suprarenal abdominal  
741 aorta sections. **I-L**, Quantifications of AAA incidence (**I**), maximal aorta diameter (**J**),  
742 elastic fiber degradation score (**K**), and dissection rate (**L**) among the 3 groups. **M**,  
743 Relative abundance of *Apoc3* in the liver. **N**, Plasma mouse-specific APOC3  
744 concentrations were measured by ELISA at the endpoint. **O**, Relative liver abundance of  
745 human APOC3. **P**, Plasma human APOC3 concentrations were determined by ELISA at  
746 the endpoint. **Q**, Body weight comparisons among the 3 groups before and at the end of  
747 the study. **R**, Systolic blood pressure comparisons among the 3 groups before and at  
748 the end of the study. Data are presented as circles/dots and Mean  $\pm$  SEM or Mean only.  
749 Statistical analyses were conducted as follows: One-way ANOVA followed by Sidak post

750 hoc analysis for **B, C, D, E**, day 3 of **F, M, N, R**; Kruskal-Wallis test followed by Dunn's  
751 post hoc analysis for day 0 and 28 of **F, J, K, O, P, Q**; Chi-Squared test for **I, L**. Scale  
752 bars: 1 mm in **G**, 50  $\mu$ m in **H**. SBP, systolic blood pressure; NEFA, non-esterified fatty  
753 acids; #,  $P < 0.005$  of the comparison of Ctr and WT group. \*,  $P < 0.005$  of the  
754 comparison of Ctr and ASO group.

755

756 **Fig. 6: Administration of *Angptl3* ASO prevents AAA formation in *Apoe*-deficient**  
757 **mice.**

758 **A**, Design of the *Angptl3* ASO study in male *Apoe*-deficient mice. Ten-week-old male  
759 *Apoe*-deficient mice were given a subcutaneous injection of *Angptl3* ASO (10 mg/kg; n =  
760 13) or scrambled ASO (n = 12). After 3 days, mice were infused with AngII (1,000  
761 ng/kg/min) for 25 days. Three more injections were administered on days 7, 14, and 21.  
762 At the end of the study, aortas, livers, and plasma were harvested. **B**, Relative  
763 abundance of *Angptl3* mRNA in the liver. **C-D**, Plasma ANGPTL3 protein concentrations  
764 (**C**), and non-esterified fatty acids (**D**) at the endpoint. **E**, Plasma triglycerides (TG)  
765 levels on days 0, 3, and 28. **F**, Plasma total cholesterol (TC) concentrations on days 3  
766 and 28. **G**, Systolic blood pressure before and after AngII infusion. **H**, Body weight  
767 changes. TG (**I**) and cholesterol (**J**) concentrations of size exclusion chromatography  
768 fractionated plasma from animals (n = 4 in the control group, n = 4 in the *Angptl3* ASO  
769 group) determined by enzymatic assays. Fractions 8 to 11 contained VLDL, fractions 12  
770 to 17 contained IDL and LDL, and fractions 22 to 25 contained HDL. **K**, Representative  
771 aortic images from the 2 groups. **N-O**, Quantification of AAA incidence (**N**) and maximal  
772 aortic diameter (**O**). **P**, Relative liver mRNA abundance of genes related to VLDL  
773 production (*Apob*, *Mttp*, *Srebp1c*, *Scd*, *Fasn*), TG lipolysis (*Apoc2*, *Apoc3*, *Apoa5*, *Lpl*),  
774 and TC regulation (*Pcsk9*, *Ldlr*, *Lrp1*). Data are presented as circles/dots and/or Mean  $\pm$   
775 SEM. Statistical analyses were conducted as follows: Student's t-test for **B, C**, day 0  
776 and 28 of **E**, day 28 of **F**; Mann-Whitney U test for **D**, day 3 of **E** and **F, O**; One-way  
777 ANOVA followed by Sidak post hoc analysis for **G**; Chi-Squared test for **N**; Student's t-  
778 test or Mann-Whitney U test for **P**. Scale bars: 1 mm in **K**. SBP, systolic blood pressure;  
779 NEFA, non-esterified fatty acids.



**Figure 1**

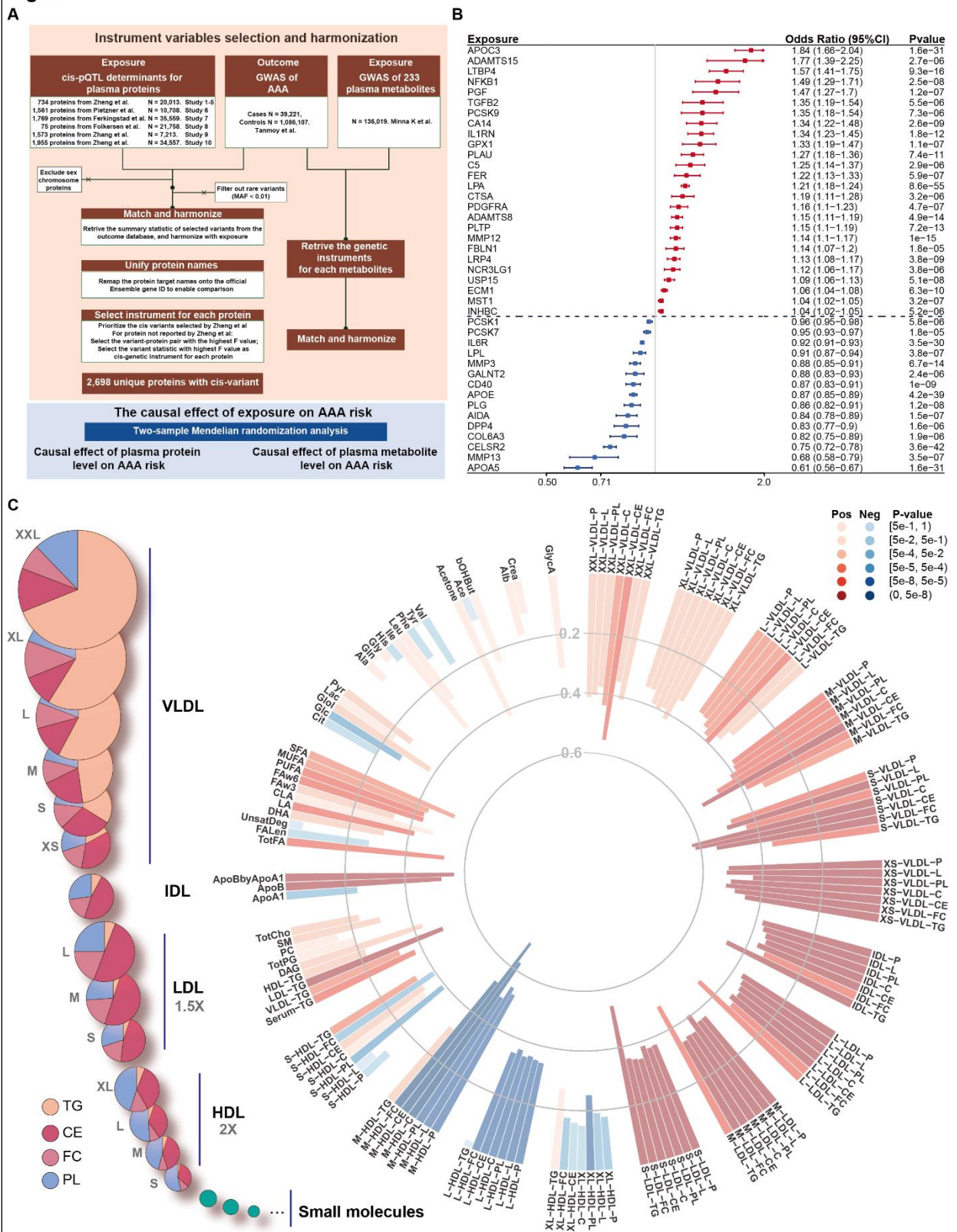


**Figure 2**

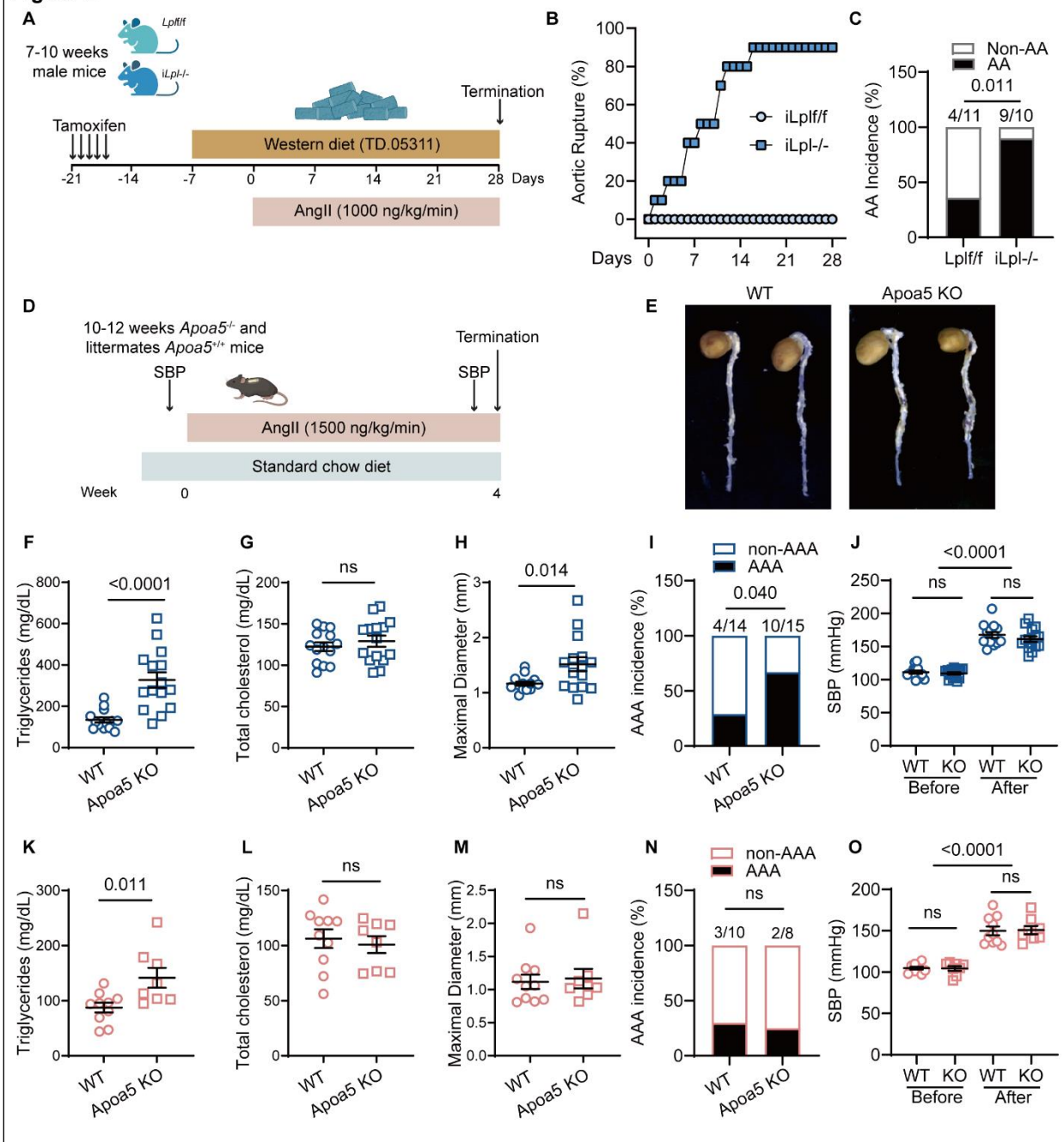


**Figure 3**

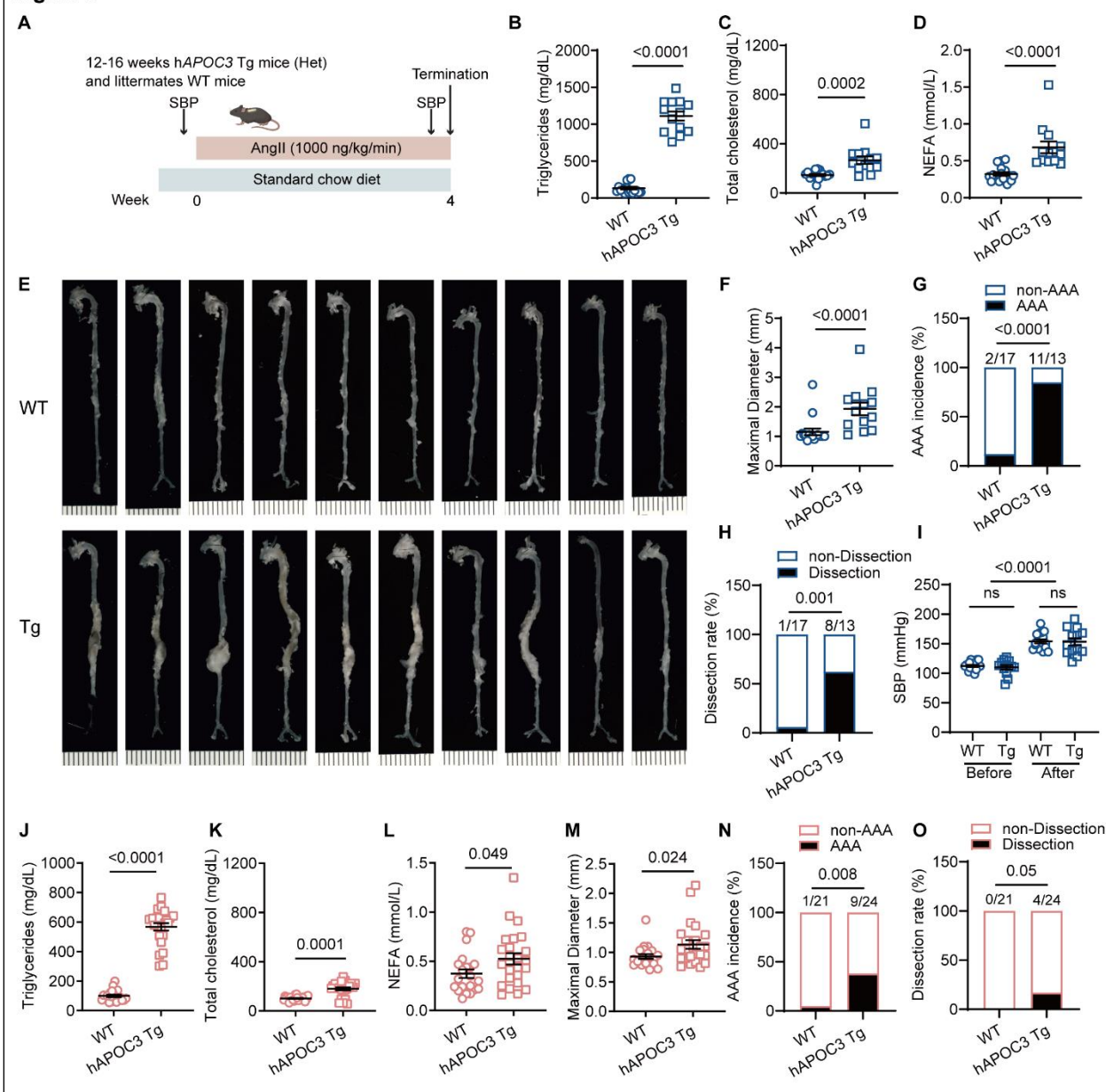


**Figure 4**

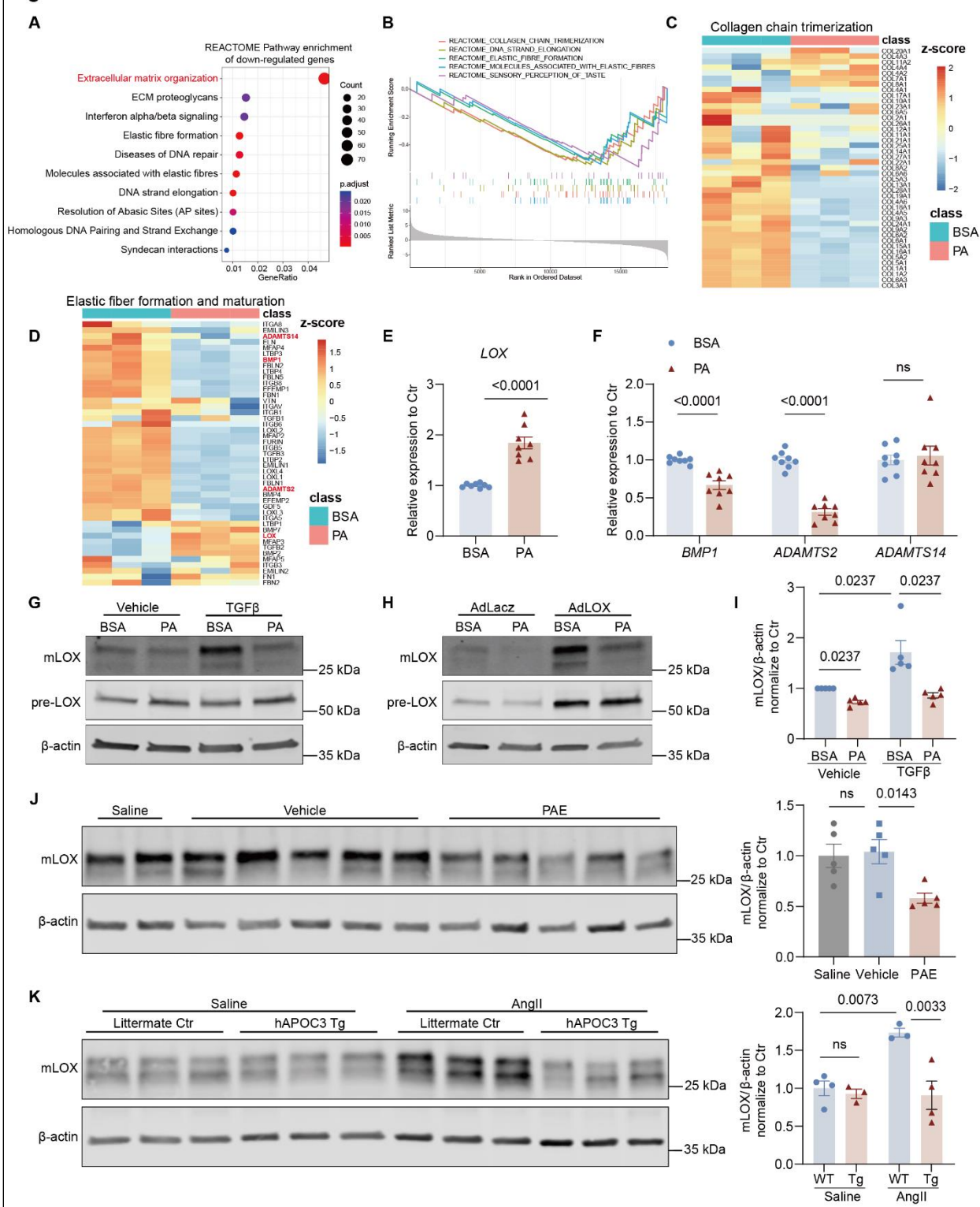


**Figure 5**

